ChemPubSoc Europe

DOI: 10.1002/cssc.201600757

CHEMSUSCHEM Full Papers

VIP *Very Important Paper*

Shape-selective Valorization of Biomass-derived Glycolaldehyde using Tin-containing Zeolites

Søren Tolborg,[a, b] Sebastian Meier,[a] Shunmugavel Saravanamurugan,[a] Peter Fristrup,[a] Esben Taarning,[b] and Irantzu Sádaba*[b]

A highly selective self-condensation of glycolaldehyde to different C_4 molecules has been achieved using Lewis acidic stannosilicate catalysts in water at moderate temperatures (40–100 °C). The medium-sized zeolite pores (10-membered ring framework) in Sn-MFI facilitate the formation of tetrose sugars while hindering consecutive aldol reactions leading to hexose sugars. High yields of tetrose sugars (74%) with minor amounts of vinyl glycolic acid (VGA), an α-hydroxyacid, are obtained using Sn-MFI with selectivities towards C_4 products reaching 97%. Tin catalysts having large pores or no pore structure (Sn-Beta, Sn-MCM-41, Sn-SBA-15, tin chloride) led to lower selectivities for C_4 sugars due to formation of hexose sugars. In the case of Sn-Beta, VGA is the main product (30%), illustrating differences in selectivity of the Sn sites in the different frameworks. Under optimized conditions, GA can undergo further conversion, leading to yields of up to 44% of VGA using Sn-MFI in water. The use of Sn-MFI offers multiple possibilities for valorization of biomass-derived GA in water under mild conditions selectively producing C_4 molecules.

Introduction

Glycolaldehyde (GA), a two-carbon monosaccharide, has the potential to become a valuable biomass-derived platform chemical. It is currently obtained in high yields in supercritical water or as a main component of bio-oil, and other processes to efficiently transform sugars to GA in high yields are currently being developed.[1]

GA can be catalytically converted into many interesting chemicals. For example, ethylene diamine or ethanolamine, with applications in polymer production and pharmaceuticals, can be produced by direct amination.[2] Glyoxal, glycolic acid, or glyoxylic acid can be obtained by oxidation, whereas ethylene glycol can be produced by reduction (hydrogenation). Alternatively, the aldehyde functionality can be employed in C–C bond formations, such as aldol condensations.[3] The self-condensation of GA, leading to the formation of tetrose sugars, permits the production of uncommon and expensive sugars. The tetroses currently have limited potential uses, for example within pharmaceutical treatments,[4] but increased availability could provide a new platform for biomass-derived products. Especially products that are otherwise difficult to access from cheaper pentose and hexose sugars are attractive. The sweetener erythritol, for example, is currently obtained by fermentation of glucose and sucrose, but could be obtained through hydrogenation of the tetrose sugars.[5] Under hydrothermal alkaline conditions the monomer lactic acid has also been obtained, by way of aldol condensation and subsequent conversion of GA.[6] Similarly, several interesting products have been obtained by employing Lewis-acid catalysts, including the α-hydroxyacids lactic acid/methyl lactate (LA/ML), methyl vinyl glycolate (MVG), and methyl 4-methoxy-2-hydroxy-3-butenoate (MMHB).[7] In addition to these, the formation of the pharmaceutical precursor α-hydroxy-γ-butyrolactone (HBL) from smaller sugars (C_1 to C_3) has been reported.[3,7b,8]

The condensation of GA with small oxygenates such as formaldehyde (FA) has long been considered a plausible pathway in the abiotic synthesis of sugars.[9] In the catalytic self-condensation of GA, the challenge is to control the selectivity towards tetrose sugars while avoiding the formation of hexoses (Scheme 1). Various strategies have been utilized to control the aldol condensation of smaller sugars towards the desired condensation products. The most common catalysts used in this reaction include bases,[10] amino acids,[11] and peptides.[12] Inorganic hydroxides such as calcium hydroxide have been extensively studied, alongside various minerals such as borates,[13] silicates,[14] and phosphates.[9b] A combined yield of tetrose derivatives of 86% was obtained using GA and borates at moderate temperatures (65 °C).[13b]

One of the major advantages of zeolite catalysis is the ability to control product selectivity by choosing materials with suitable pore sizes.[15] Zeolites have previously been used with

[a] S. Tolborg, Dr. S. Meier, Dr. S. Saravanamurugan,[+] Dr. P. Fristrup
Department of Chemistry
Technical University of Denmark
Kemitorvet, 2800-Kgs. Lyngby (Denmark)

[b] S. Tolborg, Dr. E. Taarning, Dr. I. Sádaba
New Business R&D
Haldor Topsøe A/S
Haldor Topsøes Allé 1, 2800-Kgs. Lyngby (Denmark)
E-mail: irsz@topsoe.dk

[+] Current address:
Center of Innovative and Applied Bioprocessing (CIAB)
Mohali, 160071-Punjab (India)

Supporting Information and the ORCID identification numbers for the authors of this article can be found under http://dx.doi.org/10.1002/cssc.201600757.

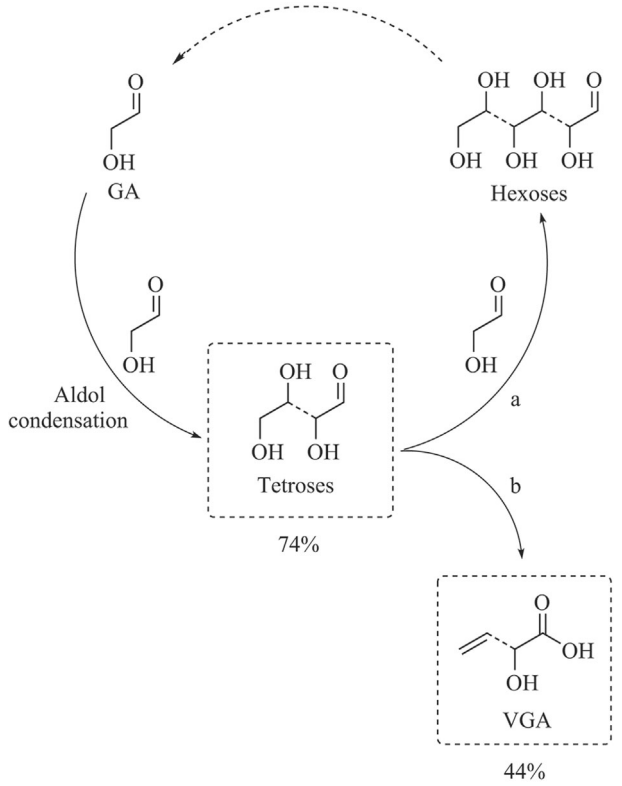

Scheme 1. Schematic representation of the conversion of hexose sugars to the C_2 sugar glycolaldehyde (reported elsewhere) followed by aldol condensation to the tetrose sugars and subsequent aldol condensation to hexoses (a) or isomerization and β-elimination to vinyl glycolic acid (VGA, b).

some success to control the condensation of formaldehyde to selectively form the C_3 sugar 1,3-dihydroxyacetone.[16] Recently, solid Lewis-acid catalysts have been shown to achieve high selectivity in aldol and cross-aldol reactions for the formation of a range of chemicals.[3,7a,17] Different micro- and mesoporous metallosilicates are available through either direct hydrothermal synthesis or post-synthetic procedures, including the tin-containing zeotypes Sn-Beta, Sn-MFI, Sn-USY, and Sn-MWW, as well as the ordered amorphous Sn-MCM-41 and Sn-SBA-15.[18] The choice of framework has proven important for carbohydrate conversion. For the isomerization of sugars, the large channels (12-membered ring, with an average diameter of 6.5–7 Å) in Sn-Beta could easily facilitate the conversion of all monosaccharides (C_3 to C_6). In contrast, the medium-size channels (10-membered ring, with an average diameter of 5.5–6 Å) of the MFI framework were found suitable for the conversion of triose sugars, while the reactions of pentose and especially hexose sugars was much slower, owing to the difference in size of the substrates.[19] Recently, such shape selectivity was identified in the conversion of tetrose sugars, where different catalyst structures lead to significantly different product distributions.[20] With this in mind, the objective of the present study was the selective formation of tetrose sugars from GA in water under mild reaction conditions, investigating the influence of catalyst framework on the product selectivity.

We show here that the medium-pore zeolite Sn-MFI catalyzes the formation of tetrose sugars and vinyl glycolic acid with high selectivity (up to 98%) resulting in a combined yield of C_4 products of up to 80% (at 90% conversion), while avoiding the formation of hexoses (<2%). Owing to the mild reaction conditions (80 °C), the catalyst shows good reusability over several cycles.

Results and Discussion

Catalyst preparation and characterization

Crystalline (MFI and Beta) zeolites and ordered amorphous (MCM-41 and SBA-15) silicates were chosen for their differences in channel diameter, ranging from 5.5 Å (MFI) and 6.5 Å (Beta) to ca. 30 Å (MCM-41) and ca. 40 Å (SBA-15).[20] All tin-containing catalysts (MFI, Beta, MCM-41, and SBA-15) were prepared by direct hydrothermal synthesis, following procedures described in the literature.[18a–c,21] Sn-MFI was prepared following two different approaches: i) utilizing hydroxide ions as mineralizing agents, yielding the catalyst designated Sn-MFI (100, OH^-); or ii) using fluoride ions, yielding the catalyst designated Sn-MFI (400, F^-).[18a] The number in parentheses is the nominal Si/Sn ratio.

The structure and physical properties of the micro- and mesoporous materials were confirmed by X-ray diffraction and N_2-adsorption/desorption measurements (see Supporting Information, Figures S1–S3, and Table 1). The prepared Beta and MFI zeotypes all showed high crystallinity of their respective zeolite phases (see Figure S1). As expected, the morphology and size of the prepared Sn-MFI catalyst crystals were highly influenced by the preparation method. Scanning electron microscopy (SEM) revealed that the hydroxide route yielded small (0.5–1.5 μm), spherical crystals, whereas the fluoride route resulted in much larger, prism-shaped crystals (see Figure 1a–b), explaining the differences in textural properties seen in Table 1, entries 1–2. The expected capped square bipyramidal morphology was found for the unseeded Beta crystals (Figure 1c).[21] No discernible morphology was observed for Sn-MCM-41 and Sn-SBA-15 (not shown).[18c]

For the amorphous materials, low-angle X-ray diffraction (0°–5° 2θ) showed the characteristic (100), (110), and (200) reflections appearing as a consequence of diffraction from the hexagonally ordered structure (Supporting Information, Fig-

Table 1. Structure and physical properties of the catalysts.[a]

Entry	Sample	Si/Sn ratio[a] (elemental analysis)	Surface area [$m^2 g^{-1}$]		Pore volume [$mL g^{-1}$]	
			S_{BET}[b]	S_{micro}	V_{total}	V_{micro}[c]
1	Sn-MFI (100, OH^-)	82	404	273	0.25	0.14
2	Sn-MFI (400, F^-)	383	377	337	0.20	0.13
3	Sn-Beta (150)	186	492	395	0.28	0.21
4	Sn-MCM-41 (150)	148	857	–	1.09	–
5	Sn-SBA-15 (200)	271	918	111	1.09	0.06

[a] Determined by ICP analysis. [b] Brunauer–Emmett–Teller (BET) surface area. [c] Micropore volume calculated using the *t*-plot method.

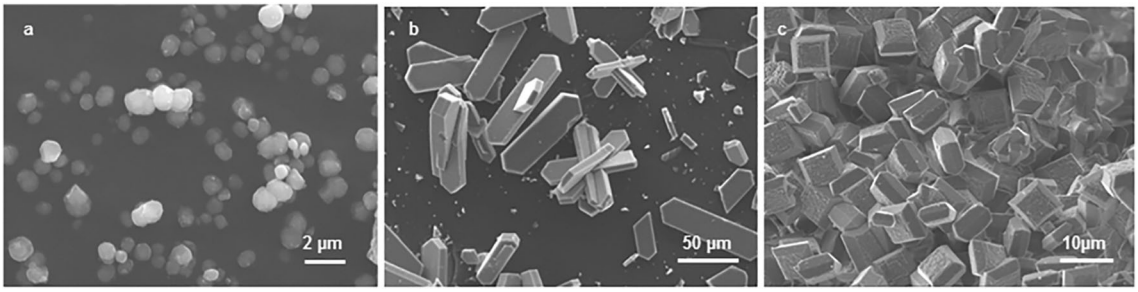

Figure 1. Electron microscope images of a) Sn-MFI (100, OH^-), b) Sn-MFI (400, F^-) and c) Sn-Beta (150, F^-).

ure S2).[18c,22] The measured angles correspond to d_{100} spacings of ca. 40 and ca. 100 Å for Sn-MCM-41 and Sn-SBA-15, respectively. The large pore volume and surface area anticipated for these two types of materials were confirmed by N_2 adsorption/desorption measurements showing total surface areas of ca. 900 $m^2 g^{-1}$ and a pore volumes of ca. 1.2 $mL g^{-1}$ for both materials (Table 1).

Elemental analysis was performed to evaluate the metal content in the material (see Table 1). For both tin-containing MFI zeolites, a slightly higher Si/Sn ratio was obtained than expected based on the nominal values, pointing at some loss of silicon during synthesis. Incorporation of tin for Sn-MCM-41 (Si/Sn = 148) was found to be close to the nominal values (150) (Table 1, entry 4). For the rest of the catalysts (Table 1, entries 3 and 5), the Si/M ratios were slightly higher than the nominal ratio, meaning that a loss of metal occurred during synthesis.

Condensation of glycolaldehyde with different catalysts

As expected in consecutive reactions, products are not stable since they can continue reacting. Therefore, selectivity was found to be highly dependent on the degree of conversion. As a consequence, catalysts are henceforth compared as a function of conversion rather than by showing the conventional kinetics (yields over time can be found in the Supporting Information, Table S1 and Figure S4). This depiction allows the comparison of different catalysts under equivalent conditions, regardless of the intrinsic activity of the catalysts due to metal loading.

Figure 2 shows the combined yield of tetrose sugars as a function of conversion for several Lewis-acid and -base catalysts. Apart from the stannosilicates, materials without a defined pore structure (zirconia, Amberlyst A21) and homogeneous catalysts such as $SnCl_4 \cdot 5H_2O$ were used to probe the effect of the pore structure. A weak base resin, Amberlyst A21, containing dimethyl amino functional groups, was used as a reference for base-catalyzed aldol condensation. For some of the catalysts (Sn-MCM-41, Sn-SBA-15, and ZrO_2), a high selectivity (near 100%) towards the desired aldol products is only obtained as long as conversion is kept low (< 20%), quickly decreasing with increased conversion. The tested catalysts fall into two different groups in terms of product yield (Figure 2): for one group (marked in blue) the tetroses are merely intermediates, whereas the other group (marked in green) provides extraordinarily high selectivity (up to 96%) for tetrose sugars. Sn-MFI (100, OH^- and 400, F^-) and Amberlyst A21 are clearly the preferred catalysts for aldol condensation of GA, leading to high tetrose yields of up to 74%. In the three cases the tetrose sugar yield drops drastically above 80% conversion. This trend was independent of the temperature (40–100 °C, Supporting Information Table S4 and Figure S5). It is, however, evident from Figure 2 that Sn-MFI (100, OH^-) maintains selectivity for tetrose sugar formation to higher conversion values than all the other selective catalysts tested herein (dashed lines). As a result, Sn-MFI (100, OH^-) reaches a yield of 74% of tetrose sugar after only 30 mins (Figure S5) at 76% conversion before a drop in tetrose sugar yield is observed. Clearly, with an increase in conversion the probability for an aldol reaction between two GA molecules diminishes and instead alternative reaction pathways are preferred (discussed later).

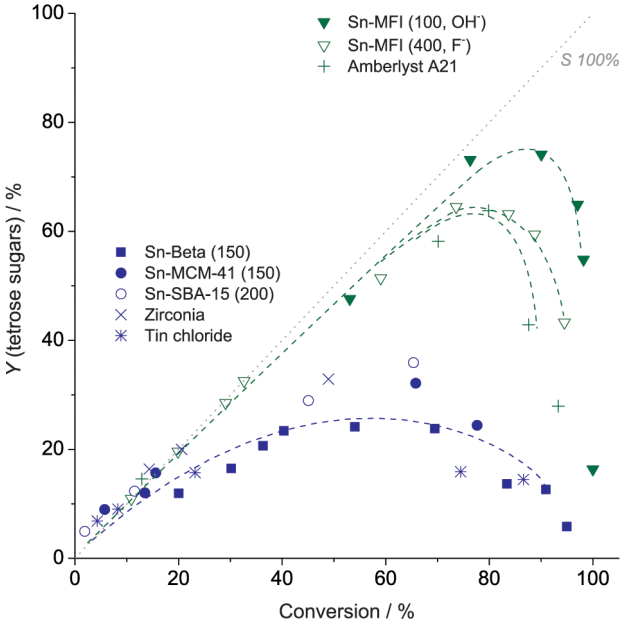

Figure 2. Yield of tetrose sugars obtained with different catalysts from glycolaldehyde as a function of conversion. The grey dotted line represents a selectivity of 100%. Reaction conditions: 80 °C, 5 wt% glycolaldehyde (dimer) in water, 0.075 g of catalyst, 2.5 g of water, reaction times 1–48 h (corresponding data can be found in Table S1).

When comparing the stability of the Sn-MFI catalyst and the basic resin, significant differences were observed during reuse

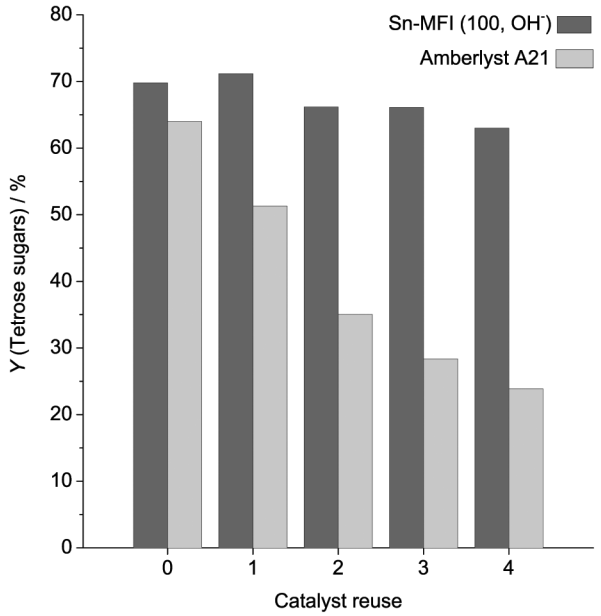

Figure 3. Yields of tetrose sugars obtained from glycolaldehyde when reusing Sn-MFI (100, OH^-) or Amberlyst A21. The catalysts were washed repeatedly with water and dried over night at 80 °C between runs. Reaction conditions: 80 °C, 5 wt% glycolaldehyde in water, substrate-to-catalyst ratio of 1.7, 2 h, 600 rpm stirring. Data and carbon balances can be found in Table S2.

experiments of Amberlyst A21 and Sn-MFI (100, OH^-) after washing of the used catalyst with water (Figure 3). The tetrose yield was found to be almost constant in the case of Sn-MFI (100, OH^-), with only a small decrease from 69 to 65% over several consecutive cycles, demonstrating good catalyst stability. For Amberlyst A21, a deactivation of the catalyst was observed, with a decrease of tetrose yield from 64 to 25% over five cycles. Both catalysts generally require regeneration in-between uses; for zeolites, calcination at temperatures over 500 °C is often performed to remove carbonaceous species trapped within the pore system and Amberlyst A21 can be treated in a flow of aqueous base to regenerate basicity. It is interesting to note that in Figure 3, only thorough washing and drying (80 °C) overnight was done to regenerate the catalysts. For Sn-MFI, washing of the zeotype catalyst was found to be fully sufficient in removing almost all carbonaceous species accumulated within the pore system. Thermogravimetric measurements of a spent Sn-MFI catalyst after the washing step revealed a negligible mass loss of 2.9 wt% (Supporting Information, Figure S6). In the case of Amberlyst A21, a regeneration procedure based on the conditions provided by the supplier (DOW) was attempted. The regeneration involved exposing the catalyst to different concentrations of NH_4OH for 1 h, followed by thorough washing to remove excess base adsorbed to the resin. Nevertheless, the regeneration procedures used did not improve the catalytic activity in the consecutive cycles (Supporting Information, Figure S7).

Regarding the formation of other byproducts in the reaction, Table 2 summarizes the yield of all products detected for the different catalysts at comparable conversion levels (70±6%). Sn-MFI (100, OH^-) showed the highest tetrose sugar selectivity (96%) and carbon balance (99%) followed by Sn-MFI (400, F^-) and Amberlyst A21 (entries 1, 2, and 7, respectively). The main by-products identified in the reaction are formed by further conversion of the formed tetrose sugars by (i) consecutive condensations with GA leading to the formation of hexoses, or (ii) dehydration and 1,2-hydride shifts to form vinyl glycolic acid (VGA) and HBL.[7a,23] Stannosilicate materials (Sn-MFI, Sn-Beta, Sn-MCM-41, and Sn-SBA-15) have been reported to catalyze the isomerization of sugars, including tetrose sugars.[7a,18c] As a result, the distribution of tetrose isomers changes over time towards erythrulose (ERU; Supporting Information, Figure S8a–d).[24] For Amberlyst A21, isomerization is hardly observed and the primary tetrose isomer observed is threose (THR) (Figure S8e). The use of homogeneous tin chloride (Table 2, entry 6) resulted in some formation of tetrose sugars (16%) at 74% conversion. Several volatile unidentified products with high boiling points were observed on CG, resulting in a lower mass balance (45%). Tin chloride could potentially precipitate under the reaction conditions to yield tin hydroxide species with a different reactivity compared with the other tested materials, as observed by Dusselier et al.[7b] In line with previous reports, no formation of tetrose sugars was observed using SnO_2-Beta zeolites (Sn-Beta prepared using SnO_2 as the tin source). From this it can be concluded that tin incorporated in the zeolite must be the active sites for the aldol condensation as neither tin nor the silicious framework show any activity in the reaction (Supporting Information, Table S3).[21,25]

Table 2. Comparison of product distribution using different catalysts at comparable conversion levels (70±6%).[a]

Entry	Catalyst	*t* [h]	Conversion [%]	Product distribution[b] [%]					Selectivity (total C_4) [%]	Carbon balance [%]
				THR	ERY	ERU	VGA + HBL	hexose sugars		
1	Sn-MFI (100, OH^-)	0.5	76	19	15	39	1	1	96	99
2	Sn-MFI (400, F^-)	6.5	74	19	16	30	2	1	88	95
3	Sn-MCM-41 (150)	24	66	11	5	16	3	7	49	76
4	Sn-SBA-15 (200)	48	65	12	8	15	–	6	55	78
5	Sn-Beta (150)	3	69	6	1	16	16	5	49	75
6	$SnCl_4{\cdot}5H_2O$[c]	24	74	9	4	3	-	3	21	45
7	Amberlyst A21	2	70	35	14	9	–	4	83	92

[a] Reaction conditions: 0.125 mg glycolaldehyde dimer, 0.075 g catalyst, 2.5 g demineralized water, 80 °C, 600 rpm, 0.25–48 h. [b] Yield (carbon percent) of threose (THR), erythrose (ERY), erythrulose (ERU), vinyl glycolic acid (VGA), and hexose sugars from glycolaldehyde (GA). [c] 0.025 g of catalyst used.

Byproduct formation

From data in Table 2 shown at 65–75% conversion, it is clear that all the catalysts tested form small amounts of hexose sugars by additional aldol condensation reactions between tetrose sugars and GA. When comparing the formation of hexose sugars as a function of conversion (Figure 4), it can be seen that all catalysts except Sn-MFI form hexoses already at low conversion, increasing up to a yield of 8–10% at almost full conversion. Despite achieving high selectivity towards the tetrose sugars, Amberlyst A21 (Table 2, entry 7) likewise formed large quantities of hexoses, especially when approaching full conversion (up to 10%, Figure 4). Amberlyst A21 showed no formation of VGA. Sn-MCM-41 and Sn-SBA-15 (Table 2, entries 3–4) behaved similarly, resulting in modest selectivities towards the tetrose sugars with a similar formation of hexose sugars (up to 6%, Figure 4) and additional formation of low yields of VGA (up to 4%, Table S1). On the other hand, Sn-MFI zeolites both maintained a low formation of larger sugars until a conversion of 75%, after which the yield of hexoses increased to 4%.

The similar product distribution of both Sn-MFI materials (OH^- and F^-), despite having very different crystal sizes (Figure 1), suggests that the high selectivity towards the tetrose sugars is not limited by the physical properties of the materials and is rather a result of the confined active tin sites within the narrow channels of the zeolite framework.[20] When comparing Sn-MFI and Sn-Beta, it is clear that larger products (hexose sugars) are obtained using the 12-membered ring framework of Sn-Beta (Table 2 entry 5, Figure 4). It has been shown previously that Sn-MFI shows very poor activity when hexose sugars are used as substrate, which might indicate that hexoses are too large to enter the pores.[19b] Additionally, the formation of large products that might accumulate in the pores and cavities of the MFI framework can be ruled out, because negligible amounts of carbon were left after washing in water (Figure S6). Therefore, we are led to speculate that the smaller porous system of the MFI zeolite hinders condensation of substrates larger than glycolaldehyde and that the high selectivity is a consequence of shape selectivity.[26]

To validate the formation of hexoses, we chose to analyze the reaction mixtures by multidimensional NMR because of its ability to distinguish similar analytes and isomers, especially hexoses.[27] Figure 5 shows the anomeric region of a highly resolved ^1H–^{13}C NMR region for reactions using Sn-MFI (400, F^-) (Figure 5a) and Amberlyst A21 (Figure 5b) run to ca. 85% conversion in D_2O. As expected, both catalysts form large quantities of aldotetroses. ERY and THR are detected in this region as α- and β-furanose forms in addition to hydrated open-chain forms (Figure 5). All eight aldohexoses (allose, altrose, glucose, mannose, gulose, idose, and talose) are detected for Amberlyst A21 (Figure 5b). In contrast, only minor amounts of mannose, glucose and gulose are detectable for the Sn-MFI catalyzed re-

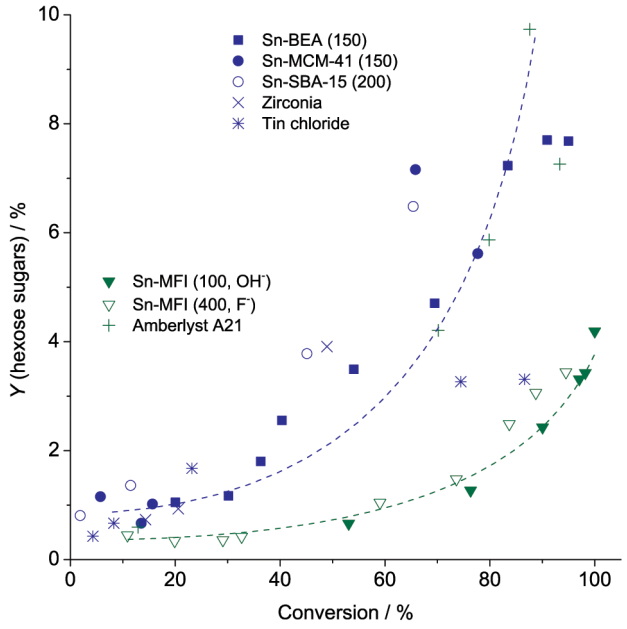

Figure 4. Yield of C_6 sugars obtained with different catalysts from pure glycolaldehyde as a function of conversion. Reaction conditions: 80 °C, 5 wt% glycolaldehyde (dimer) in water, 0.075 g of catalyst, 2.5 g of water, reaction times 0.25–48 h (corresponding data in Table S1).

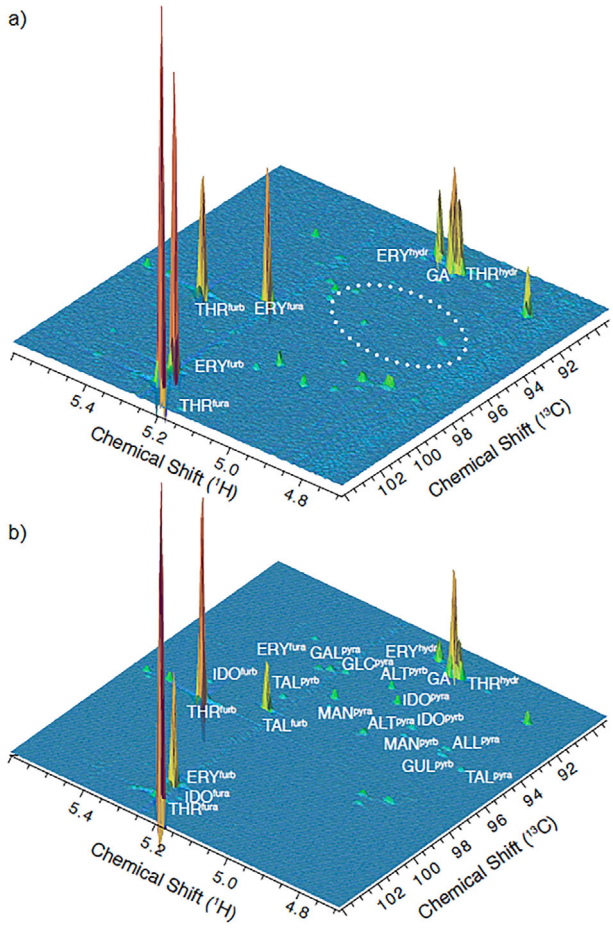

Figure 5. ^1H-^{13}C HSQC spectra of hemiacetal groups in the reaction mixture produced by the catalytic conversion of GA dimer (80 °C, D_2O) using a) Sn-MFI (100, OH^-) and b) Amberlyst A21. Samples are measured at ~85% conversion. Compounds were identified by reference compounds and by homo- and heteronuclear NMR assignment spectra recorded on the mixture. Information on abbreviations used is available as Supporting Information.

action (Figure 5a). These findings confirm that all stereoisomers of hexose sugars can be formed from consecutive aldol reactions at high conversion, whilst the confinement in narrow pores of Sn-MFI restricts hexose formation.

In addition to the formation of larger sugars, the formed tetroses can undergo dehydration and 1,2-hydride shift to yield α-hydroxyacid vinyl glycolic acid (VGA) and α-hydroxy-γ-butyrolactone (HBL). This group of chemicals has been obtained from a range of different sugars (C_3–C_6) with promising application in the formulation of new materials.[7a,23,28] For example, using either condensation or metathesis, VGA has been shown to form functional polyesters and polyamides.[7b,29] In a previous study by the group of Sels, several alkyl ester analogues of VGA were formed using $SnCl_4{\cdot}5H_2O$ as catalyst in alcohol as solvent. Under these conditions, methyl-4-methoxy-2-hydroxy-3-butanoate (MMHB) was the main product, with a maximum yield of 55%.[7b] This molecule does not contain the vinyl group characteristic for VGA. From the data presented in Table 2, it is clear that not all the catalysts tested form HBL and VGA in significant amounts. The most active catalysts for HBL and VGA formation are Sn-MFI and Sn-Beta. The results also suggest that the selectivity towards the different co-products is not only affected by the type of catalyst, but also by the concentration of GA in the medium. At the beginning of the reaction, the reaction medium is rich in GA and the possibility for two molecules of GA reacting with each other is high. With diminishing GA substrate and tetrose sugar formation, reactions can progress by formation of hexose sugars or further conversion of tetroses to VGA becomes more likely. This effect was also observed when the starting concentration of GA was changed (Supporting Information, Table S5 and Figure S9). At low GA concentrations, VGA is formed in higher relative yields (10% vs 3%, for initial concentrations of GA of 2% and 8%, respectively, after 2 h, using the same amount of catalyst). Bearing this difference in selectivity in mind, we tried to optimize the reaction conditions for the production of VGA.

Sn-Beta and Sn-MFI were found to form significant amounts of VGA in water, leading to yields of 39% using Sn-MFI (100, OH^-) and 30% using Sn-Beta (150) after 48 h (Figure 6 and Supporting Information, Figure S10). When the amount of Sn-MFI catalyst was increased, the dehydration reaction was favored and the yield of VGA reached 44% (Supporting Information, Table S6) at 100 °C after 4.5 h. This is the highest VGA yield reported hitherto in water. In the case of Sn-Beta, similar conditions lead to the formation of up to 33% HBL and 27% VGA after 48 h at 80 °C to give a combined yield of ~60% (Figure 6).

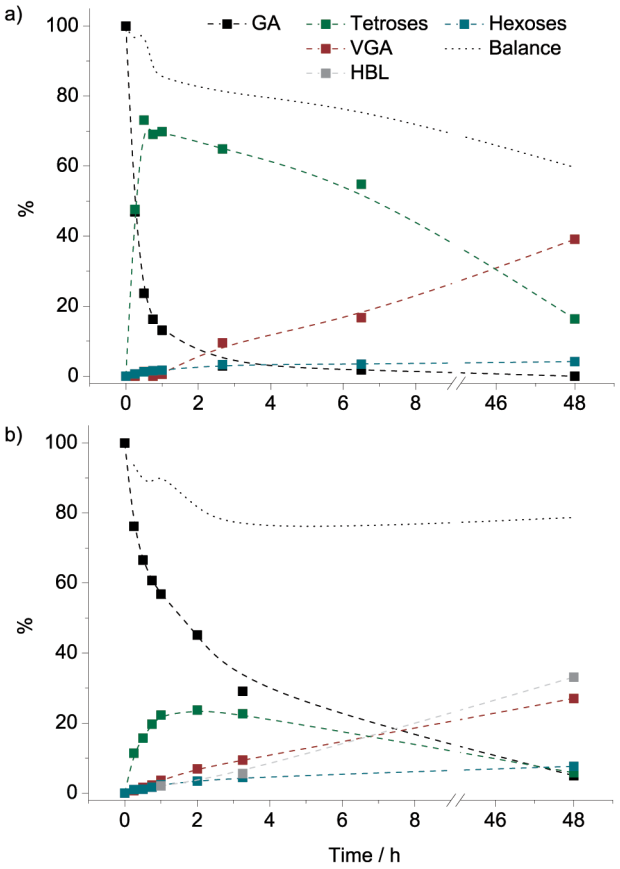

Figure 6. Conversion of glycolaldehyde over time using a) Sn-MFI (100, OH^-) and b) Sn-Beta (150). Reaction conditions: 80 °C, 5 wt% glycolaldehyde in water, 0.075 g of catalyst, 2.5 g of water, 0–48 h. Data can be found in Table S1.

Conclusions

The valorization of biomass-derived glycolaldehyde (GA) using tin-containing zeotypes in water has potential for establishing a platform for tetrose-derived products. By exploiting the shape-selectivity of the zeolite frameworks with different pore sizes, C_4 products can be obtained with high selectivity. The main products of the reaction of GA in water using medium pore Sn-MFI as catalyst are C_4 sugars. Total yields of C_4 products of 74% were obtained with 97% selectivity after 0.5 h at 80 °C in water. The formation of hexose sugars by consecutive aldol condensation reactions is minimized when the medium-pore-size zeolite MFI is used, compared to catalysts containing larger pores. We further observe that tin sites in zeolites MFI and Beta catalyze the additional transformation of tetrose sugars into vinyl glycolic acid (VGA). The reaction conditions can be tuned not only to obtain tetrose sugars in high yields and at high selectivity, but also good yields (up to 44%) of VGA can be achieved under mild conditions.

Experimental Section

Catalyst preparation

MFI zeotype materials used in this study were prepared following two different synthesis routes initially described by Mal et al.[18a] For the preparation of Sn-MFI (100, OH^-), $SnCl_4{\cdot}5H_2O$ (98%, Aldrich) was dissolved in 5 g of demineralized water and added to 15.6 g of tetraethyl orthosilicate (TEOS, 98%, Aldrich) and stirred for 30 mins. 13.4 g of tetrapropylammonium hydroxide (TPAOH, 40%, AppliChem) in 13.4 g of demineralized water was then added to the mixture and stirred for 1 h. Following this, an additional 60 g of demineralized water was added and the solution was stirred for another period of ca. 20 h, whereafter the solution was added to

a Teflon-lined autoclave and synthesized at 160 °C for 2 days under static conditions. For the preparation of Sn-MFI (400, F^-), 5.35 g of ammonium fluoride (NH_4F, Sigma–Aldrich) was dissolved in 25 g of demineralized water. To this solution, tin(IV)chloride pentahydrate ($SnCl_4{\cdot}5H_2O$, 98%, Aldrich) was dissolved in demineralized water and was added under rapid stirring. Following this, 9.8 g of tetrapropylammonium bromide (TPABr, Sigma–Aldrich) dissolved in 56 g of demineralized water was added slowly and 8.6 g of fumed silica was then added to mixture under ample stirring for 3 h. The resulting gel was transferred to a Teflon-lined autoclave and heated to 200 °C for 6 days.

Sn-Beta (Si/Sn = 150) was synthesized by following the alkali-free synthesis route described in Ref. [21]. In a typical synthesis procedure, 30.6 g of TEOS (98%, Aldrich) was added to 33.1 g of tetraethylammonium hydroxide (TEAOH, Sigma–Aldrich, 35% in water) under careful stirring. After 1 h, $SnCl_4{\cdot}5H_2O$ (98%, Aldrich) dissolved in 2 mL of demineralized water was added drop wise and stirred for 5 h. Finally, 3.1 g hydrofluoric acid (HF, Fluka, 47–51%) diluted with 1.6 g of demineralized water was added to the gel. The sample was then homogenized and transferred to a Teflon-container placed in a stainless steel autoclave and placed at 140 °C for 14 days.

The ordered mesoporous stannosilicate, Sn-MCM-41 (Si/Sn = 150), was prepared according to the route described by Li et al.[22] In a typical synthesis, 26.4 g of tetraethylammonium silicate (TMAS, Aldrich, 15–20 wt% in water, ≥99.99%) was slowly added to a solution containing 13.0 g of hexadecyltrimethylammonium bromide (CTABr, Sigma, ≥99.0%) dissolved in 38.0 g of water. This mixture was then allowed to stir for 1 h. At this point, $SnCl_4{\cdot}5H_2O$ (98%, Aldrich) and hydrochloric acid (HCl, Sigma–Aldrich, min. 37%) in 2.1 g of water was added dropwise to the solution and stirred for 1.5 h. To this solution, 12.2 g of TEOS (98%, Aldrich) was added and stirred for an additional 3 h and transferred to a Teflon-lined container placed in a stainless steel autoclave and heated to 140 °C for 15 h.

Sn-SBA-15 (Si/Sn = 200) was prepared following the synthesis route described by Ramaswamy et al.[30] Initially, 8.0 g of Pluronic P-123 (PEG-PPG-PEG polymer, M_w = 5800 g mol^{-1}) was dissolved in 60 g of demineralized water, followed by the addition of 1.0 g of hydrochloric acid (HCl, 37 wt%) in 140 g of demineralized water. The solution was then stirred for 2 h. To the synthesis mixture, 18.0 g of TEOS (98%, Aldrich) was added followed by $SnCl_4{\cdot}5H_2O$ (98%, Aldrich) dissolved in 2.0 g of demineralized water. The mixture was then stirred for 24 h at 40 °C and transferred to a Teflon-lined autoclave and heated to 100 °C for 24 h.

All prepared catalysts were recovered by filtration, washed with ample water, and dried overnight at 80 °C. The materials were finalized by calcination, heating the sample to 550 °C at 2 °C min^{-1} in static air and maintaining this temperature for 6 h.

Characterization techniques

Powder X-ray diffraction (XRD) patterns of the calcined samples were measured on an X'Pert diffractometer (Philips) using $Cu_{K\alpha}$ radiation. The elemental composition of the prepared materials was measured using inductively coupled plasma–atomic emission spectroscopy (ICP–OES) on a PerkinElmer model Optima 3000 (Varian Vista). Surface area and pore volume measurements were performed using multipoint N_2-adsorption/desorption on an Autosorb automatic surface area and pore size analyzer (Quantachrome Instruments). The total surface area of the samples was obtained using the Brunauer–Emmett–Teller (BET) method and the micropore volume was calculated by the *t*-plot method using the Autosorb3 software. Thermogravimetric analysis (TG/DSC) was performed on a TGA/DSC-1 (Mettler-Toledo).

Catalytic activity

Catalyst (0.075 g), glycolaldehyde dimer (SAFC, 0.125 g), and deionized water (2.5 g) were added in a 15 mL vial (ACE pressure tube) and heated at 80 °C under vigorous stirring (600 rpm) for between 10 min and 48 h. After finishing, the reaction was quenched in cold water and filtered samples were retrieved for analysis on an Agilent 1200-series HPLC with a BIORAD Aminex HPX-87H column and equipped with refractive index (RI) and diode array (DA) detectors operating at 65 °C using an eluent of 0.004 M H_2SO_4 solution in water at 0.6 mL min^{-1}. Unconverted glycolaldehyde and the formed tetrose sugars (erythrose, threose, and erythrulose) and larger sugars (hexoses) were quantified using the RI detector. Standard solutions of the tetrose sugars were obtained from Omicron Biochemicals, Inc. The formation of larger hexose sugars was quantified using the response factor of the aldohexose; glucose. Vinyl glycolic acid (VGA) was quantified using the DA detector at a wavelength of 210 nm with a standard (95% purity) obtained from Enamine. α-Hydroxy-γ-butyrulactone (HBL) was tentatively quantified on HPLC using the RI detector and a standard (technical grade) obtained from Aldrich. High-field NMR spectroscopy was conducted on a Bruker Avance II 800 MHz spectrometer equipped with a TCI Z-gradient CryoProbe and an 18.7 T magnet (Oxford Magnet Technology, Oxford, UK). Sufficiently ^{13}C-resolved ^{1}H–^{13}C HSQC spectra were acquired by sampling 1024 complex data points in the direct (1 H) dimension and 1024 complex data points in the indirect (13C) dimension, during acquisition times of 143 and 93 milliseconds, respectively. All spectra were recorded at 37 °C. Identification of compounds in the reaction mixture was performed by the use of pure reference standards for glycolaldehyde, tetroses, and hexoses.

Acknowledgements

The work of S.T. is funded by the Bio-Value platform (http://biovalue.dk) under the SPIR initiative by The Danish Council for Strategic Research and The Danish Council for Technology and Innovation, case number 0603-00522B. S.M. gratefully acknowledges funding by Grant 2013_01_0709 of the Carlsberg Foundation. 800 MHz NMR spectra were recorded on the spectrometer of the Danish National Instrument Center for NMR Spectroscopy of Biological Macromolecules at the Technical University of Denmark.

Keywords: aldol condensation · biomass conversion · tetrose sugars · tin · zeolites

[1] a) M. Sasaki, K. Goto, K. Tajima, T. Adschiri, K. Arai, *Green Chem.* **2002**, *4*, 285–287; b) D. Mohan, C. U. Pittman, P. H. Steele, *Energy Fuels* **2006**, *20*, 848–889; c) R. Vinu, L. J. Broadbelt, *Energy Environ. Sci.* **2012**, *5*, 9808–9826.

[2] W. Mägerlein, J. P. Melder, J. Pastre, J. Eberhardt, T. Krug, M. Kreitschmann, US20120271068A1, **2012**.

[3] S. Van de Vyver, Y. Román-Leshkov, *Angew. Chem. Int. Ed.* **2015**, *54*, 12554–12561; *Angew. Chem.* **2015**, *127*, 12736–12744.

[4] R. J. Jariwalla, US 20040092549A1, **2001**.

[5] R. Ooms, M. Dusselier, J. A. Geboers, B. Op de Beeck, R. Verhaeven, E. Gobechiya, J. A. Martens, A. Redl, B. F. Sels, *Green Chem.* **2014**, *16*, 695–707.

[6] a) H. Kishida, F. Jin, X. Yan, T. Moriya, H. Enomoto, *Carbohydr. Res.* **2006**, *341*, 2619 – 2623; b) X. Yan, F. Jin, K. Tohji, A. Kishita, H. Enomoto, *AIChE J.* **2010**, *56*, 2727 – 2733.

[7] a) M. S. Holm, Y. J. Pagán-Torres, S. Saravanamurugan, A. Riisager, J. A. Dumesic, E. Taarning, *Green Chem.* **2012**, *14*, 702 – 706; b) M. Dusselier, P. Van Wouwe, S. De Smet, R. De Clercq, L. Verbelen, P. Van Puyvelde, F. E. Du Prez, B. F. Sels, *ACS Catal.* **2013**, *3*, 1786 – 1800.

[8] a) S. Yamaguchi, T. Matsuo, K. Motokura, Y. Sakamoto, A. Miyaji, T. Baba, *ChemSusChem* **2015**, *8*, 853 – 860; b) S. Yamaguchi, T. Matsuo, K. Motokura, A. Miyaji, T. Baba, *ChemCatChem* **2016**, *8*, 1386 – 1391.

[9] a) A. N. Simonov, L. G. Matvienko, O. P. Pestunova, V. N. Parmon, N. A. Komandrova, V. A. Denisenko, V. E. Vas'kovskii, *Kinet. Catal.* **2007**, *48*, 550 – 555; b) A. N. Simonov, O. P. Pestunova, L. G. Matvienko, V. N. Snytnikov, O. A. Snytnikova, Y. P. Tsentalovich, V. N. Parmon, *Adv. Space Res.* **2007**, *40*, 1634 – 1640; c) I. Delidovich, A. Simonov, O. Pestunova, V. Parmon, *Kinet. Catal.* **2009**, *50*, 297 – 303.

[10] T. Matsumoto, S. Inoue, *J. Chem. Soc. Perkin Trans. 1* **1982**, 1975 – 1979.

[11] a) A. Córdova, I. Ibrahem, J. Casas, H. Sundén, M. Engqvist, E. Reyes, *Chem. Eur. J.* **2005**, *11*, 4772 – 4784; b) J. Kofoed, J.-L. Reymond, T. Darbre, *Org. Biomol. Chem.* **2005**, *3*, 1850 – 1855.

[12] a) S. Pizzarello, A. L. Weber, *Science* **2004**, *303*, 1151; b) A. L. Weber, S. Pizzarello, *Proc. Natl. Acad. Sci. USA* **2006**, *103*, 12713 – 12717.

[13] a) A. Ricardo, M. A. Carrigan, A. N. Olcott, S. A. Benner, *Science* **2004**, *303*, 196; b) H.-J. Kim, A. Ricardo, H. I. Illangkoon, M. J. Kim, M. A. Carrigan, F. Frye, S. A. Benner, *J. Am. Chem. Soc.* **2011**, *133*, 9457 – 9468.

[14] J. B. Lambert, S. A. Gurusamy-Thangavelu, K. Ma, *Science* **2010**, *327*, 984 – 986.

[15] S. M. Csicsery, *Zeolites* **1984**, *4*, 202 – 213.

[16] a) S. Trigerman, E. Biron, A. H. Weiss, *React. Kinet. Catal. Lett.* **1977**, *6*, 269 – 274; b) H. Tajima, K. Tabata, T. Niitsu, H. Inoue, *J. Chem. Eng. Jpn.* **2002**, *35*, 564 – 568.

[17] a) J. D. Lewis, S. Van de Vyver, Y. Román-Leshkov, *Angew. Chem. Int. Ed.* **2015**, *54*, 9835 – 9838; *Angew. Chem.* **2015**, *127*, 9973 – 9976; b) Y. Wang, J. D. Lewis, Y. Román-Leshkov, *ACS Catal.* **2016**, *6*, 2739 – 2744.

[18] a) N. K. Mal, V. Ramaswamy, P. R. Rajamohanan, A. V. Ramaswamy, *Microporous Mater.* **1997**, *12*, 331 – 340; b) A. Corma, L. T. Nemeth, M. Renz, S. Valencia, *Nature* **2001**, *412*, 423 – 425; c) C. M. Osmundsen, M. S. Holm, S. Dahl, E. Taarning, *Proc. R. Soc. London Ser. A* **2012**, *468*, 2000 – 2016; d) C. Hammond, S. Conrad, I. Hermans, *Angew. Chem. Int. Ed.* **2012**, *51*, 11736 – 11739; *Angew. Chem.* **2012**, *124*, 11906 – 11909; e) Q. Guo, F. Fan, E. A. Pidko, W. N. P. van der Graaff, Z. Feng, C. Li, E. J. M. Hensen, *ChemSusChem* **2013**, *6*, 1352 – 1356; f) X. Yang, L. Wu, Z. Wang, J. Bian, T. Lu, L. Zhou, C. Chen, J. Xu, *Catal. Sci. Technol.* **2016**, *6*, 1757 – 1763.

[19] a) J. Jae, G. A. Tompsett, A. J. Foster, K. D. Hammond, S. M. Auerbach, R. F. Lobo, G. W. Huber, *J. Catal.* **2011**, *279*, 257 – 268; b) C. M. Lew, N. Rajabbeigi, M. Tsapatsis, *Microporous Mesoporous Mater.* **2012**, *153*, 55 – 58.

[20] R. De Clercq, M. Dusselier, C. Christiaens, J. Dijkmans, R. I. Iacobescu, Y. Pontikes, B. F. Sels, *ACS Catal.* **2015**, *5*, 5803 – 5811.

[21] S. Tolborg, A. Katerinopoulou, D. D. Falcone, I. Sádaba, C. M. Osmundsen, R. J. Davis, E. Taarning, P. Fristrup, M. S. Holm, *J. Mater. Chem. A* **2014**, *2*, 20252 – 20262.

[22] L. Li, C. Stroobants, K. Lin, P. A. Jacobs, B. F. Sels, P. P. Pescarmona, *Green Chem.* **2011**, *13*, 1175 – 1181.

[23] M. Dusselier, P. Van Wouwe, F. de Clippel, J. Dijkmans, D. W. Gammon, B. F. Sels, *ChemCatChem* **2013**, *5*, 569 – 575.

[24] S. Saravanamurugan, A. Riisager, *Catal. Sci. Technol.* **2014**, *4*, 3186 – 3190.

[25] M. S. Holm, S. Saravanamurugan, E. Taarning, *Science* **2010**, *328*, 602 – 605.

[26] P. B. Weisz, *Pure Appl. Chem.* **1980**, *52*, 2091 – 2103.

[27] a) M. Bøjstrup, B. O. Petersen, S. R. Beeren, O. Hindsgaul, S. Meier, *Anal. Chem.* **2013**, *85*, 8802 – 8808; b) B. O. Petersen, O. Hindsgaul, S. Meier, *Analyst* **2014**, *139*, 401 – 406.

[28] S. Tolborg, S. Meier, I. Sadaba, S. G. Elliot, S. K. Kristensen, S. Saravanamurugan, A. Riisager, P. Fristrup, T. Skrydstrup, E. Taarning, *Green Chem.* **2016**, *18*, 3360 – 3369.

[29] a) M. Dusselier, P. Van Wouwe, A. Dewaele, P. A. Jacobs, B. F. Sels, *Science* **2015**, *349*, 78 – 80; b) A. Dewaele, L. Meerten, L. Verbelen, S. Eyley, W. Thielemans, P. Van Puyvelde, M. Dusselier, B. Sels, *ACS Sustain. Chem. Eng.* **2016**, in press, DOI: 10.1021/acssuschemeng.6b00807.

[30] V. Ramaswamy, P. Shah, K. Lazar, A. V. Ramaswamy, *Catal. Surv. Asia* **2008**, *12*, 283 – 309.

Received: June 7, 2016
Revised: July 11, 2016
Published online on ■■ ■■, 0000

Zeo moduz? A highly selective self-condensation of glycolaldehyde to different C_4 molecules is achieved with Lewis-acidic stannosilicate catalysts in water at moderate temperatures. Sn-MFI (*green*) catalyzes selectively the condensation of glycolaldehyde (*black*) to C_4 sugars. Catalysts with larger pores, such as Sn-MCM-41 (*blue*) and Sn-Beta (*red*) favor the formation of hexoses. Under optimized reaction conditions, other interesting C_4-derived products are formed.

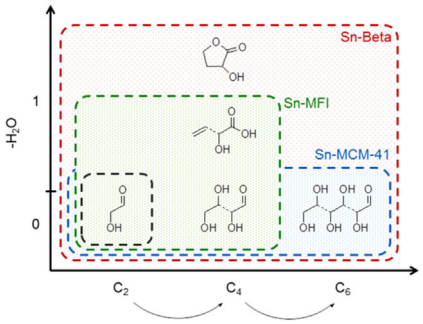

*S. Tolborg, S. Meier, S. Saravanamurugan, P. Fristrup, E. Taarning, I. Sádaba**

■■ – ■■

Shape-selective Valorization of Biomass-derived Glycolaldehyde using Tin-containing Zeolites

VIP

These are not the final page numbers! ↗↗